Feasible Operation Region of a Distribution Network Considering Thermal Constraints

Xun Jiang, Jianzhong Wu, Yue Zhou*, Wenlong Ming
School of Engineering, Cardiff University, Cardiff, UK

ABSTRACT

Conventional scenario-based analysis is not able to accurately and comprehensively evaluate the capability of a distribution network to integrate increasing demand and distributed generation (DG) due to their significant uncertainties. To solve this problem, feasible operation region (FOR) was defined and studied, which provides an effective way to obtain the whole picture of hosting capacity of a distribution network. The analytical expressions of thermal boundaries of FOR in a radial distribution network were obtained through theoretical deduction. To validate the obtained thermal boundaries, a point-wise simulation procedure for generating the cross-sections of FOR in two-dimensional power injection space was proposed. An 11kV radial distribution network from the United Kingdom Generic Distribution System (UKGDS) was used for the case study. The results show that the derived thermal boundaries can well approximate the real thermal boundaries of FOR. Moreover, these thermal boundaries of FOR are more accurate than those calculated by a method proposed in a previous study, especially when considering independent reactive power injections in the distribution network.

Keywords: feasible operation region, hosting capacity, thermal boundaries, electrical distribution networks

1. INTRODUCTION

The net zero agenda worldwide requires low carbon technologies in electricity generation and supply. To this end, large-scale low-carbon distributed generation (DG) such as wind turbines and photovoltaic panels and new electricity demand like electricity vehicles and heat pumps are expected to be integrated into distribution networks. The significant uncertainties from these generation and demand will bring great challenges to the evaluation of hosting capacity of distribution networks, which is normally based on "worst-case" analysis (e.g. cases with minimum and maximum load conditions) [1][2]. The uncertainty of DG deployment is also concerned for hosting capacity assessment. Since it is difficult to decide the scenarios of DG deployment in real-life, assessing per-node hosting capacity of distribution networks becomes a compromised method normally used by the utilities [3][4][5]. An optimistic way is to assess the maximum overall hosting capacity at all candidate locations [6]. To consider the uncertainty of DG deployment in hosting capacity analysis, Monte Carlo simulation method is commonly used [2][7][8]. However, scenario-based analysis in the existing research cannot comprehensively evaluate the hosting capacity of distribution networks.

To overcome the deficiency of conventional scenario-based methods, the operation region-based methodology has been proposed. Specifically, the security region methodology comprehensively considers network constraints and is uniquely determined for a power network with given topology and parameters [9]. Though developed and mainly applied in transmission networks, in recent years the operation region-based methodology starts to be applied to distribution networks. In [10], dispatchable region was defined to represent all the feasible operation states which satisfy the thermal and voltage constraints of distribution networks. In this study, a simulation-based approach was used to visualize the two-dimensional and three-dimensional cross-sections of the dispatchable region. However, the simulation-based method is time-consuming and the impact of the integration of DG is not considered. In [11], the analytical expressions of thermal and voltage boundaries of the steady-state security

region were derived, handling high dimensionality efficiently in a mathematical way. However, in the deduction process, the vertical component of the voltage drop was neglected and will thus have reduced performance in distribution networks with high ratio of the network resistance to the network reactance (i.e., R/X ratio). In addition, these was a lack of quantitative error analysis for these boundaries, especially when considering the impact of reactive power injections.

In this study, feasible operation region (FOR) is proposed and then applied to the analysis of hosting capacity of distribution networks. This study is targeted at the thermal constraints of distribution networks. The analytical expressions of thermal boundaries of FOR were derived from the basic relationship between the voltage drop and branch power flow. To validate the proposed analytical thermal boundaries, two-dimensional cross-sections of FOR were generated through point-wise simulation. Error analysis was also conducted for the obtained thermal boundaries and the resulting errors were compared with the errors of the boundaries calculated by a method proposed in a previous study [11].

2. CONCEPT OF FEASIBLE OPERATION REGION
2.1 Definition of feasible operation region

Feasible operation region (FOR) is defined as the set of feasible operation states of a distribution network, where the network constraints are not violated. Considering the operation states in complex power injection space, a feasible operation region can be described as follows:

$$\Omega := \left\{ x \middle| \begin{array}{c} V \in R_V, I \in R_T \\ f_{(V_0, \theta_0)}(V, \theta) = x, g(I, V, \theta) = 0 \end{array} \right\} \quad (1)$$

$\Omega \in R^{2n}$ is the feasible operation region in the power injection space, where n is the node number of the distribution network. $x := \left(P^T, Q^T\right)^T \in R^{2n}$ is the complex power injection vector in a distribution network. $f_{(V_0, \theta_0)}(V, \theta) = x$ represents the power flow equations with V_0 and θ_0 as predefined voltage magnitude and phase angle of the slack bus. $g(I, V, \theta) = 0$ represents the relationship between branch currents and node voltages, normally calculated by Ohm's law. V and I are the node voltage vector and branch current vector. R_V and R_T are the voltage constraints and thermal constraints (see (2) and (3)), respectively.

$$R_V := \left\{ V \in R^n \middle| V_i^m \leq V_i \leq V_i^M, \forall i \in N \right\} \quad (2)$$

$$R_T := \left\{ I \in R^n \middle| \left|I_{ij}\right| \leq I_{ij}^M, \forall ij \in B \right\} \quad (3)$$

2.2 Boundaries of a feasible operation region

FOR is internally void-free due to the continuity of the region restrained by (2) and (3), and the continuous nonlinear mapping of power flow equations and voltage-current relationship in (1) [9]. As a result, FOR should be enclosed by several high-dimensional surfaces against each voltage or thermal constraint. In this study, these high-dimensional surfaces are defined as the boundaries of FOR. Within the boundaries of FOR are all feasible operation states, while outside of them any operation states are infeasible. In this regard, the boundaries of FOR represent all the limits to the power injections that can be hosted by a distribution network, which can reveal the whole picture of hosting capacity for the network.

Considering the types of constraints in (2) and (3), the boundaries of FOR can be further categorized into voltage boundaries and thermal boundaries. This paper focuses on the thermal boundaries.

3. ANALYTICAL EXPRESSIONS FOR THERMAL BOUNDARIES OF A FEASIBLE OPERATION REGION

The schematic diagram of a radial distribution network is shown in Fig. 1.
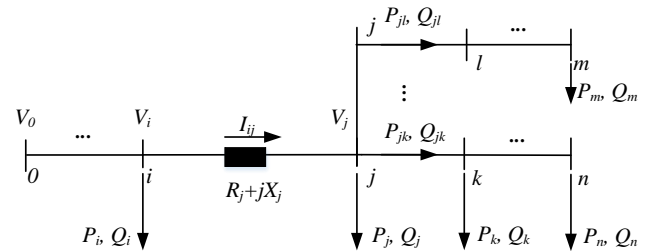

Fig. 1. A schematic diagram of a radial distribution network

For any branch ij in the distribution network in Fig. 1, the relationship between the voltage drop and the power flow on the branch can be expressed as:

$$\dot{V}_i - \dot{V}_j = \frac{P_{j,eq}R_j + Q_{j,eq}X_j}{V_j} + j\frac{P_{j,eq}X_j - Q_{j,eq}R_j}{V_j} \quad (4)$$

$\dot{V}_i$ and $\dot{V}_j$ are the voltages at the sending end and the receiving end of the branch (V_i and V_j denote the magnitude of them); R_j and X_j are the resistance and reactance of the branch; $P_{j,eq}$ and $Q_{j,eq}$ are the equivalent power loading at the receiving end node of the branch, which are expressed as:

$$\begin{cases} P_{j,eq} = P_j + \sum_{k \in A_j} P_{jk} \\ Q_{j,eq} = Q_j + \sum_{k \in A_j} Q_{jk} \end{cases} \quad (5)$$

P_j and Q_j are the active and reactive power loading at the receiving end node of the branch, while P_{jk} and Q_{jk} are the active and reactive power flow at the branch jk. A_j denotes the set of the adjoining downstream nodes of node j in the distribution network.

It is important to emphasise that comparing to the previous study [11], the imaginary part of the voltage drop equation in (4) is not ignored when deducting the boundaries for improved accuracy. Based on Ohm's law, the current of the branch ij can be obtained by

$$\dot{I}_{ij} = \frac{\dot{V}_i - \dot{V}_j}{R_j + jX_j} \tag{6}$$

From (4)-(6), the magnitude of the branch current can be expressed as:

$$\left| I_{ij} \right| = \frac{1}{V_j} \sqrt{\left(P_{j,eq}{}^2 + Q_{j,eq}{}^2 \right)} \tag{7}$$

If the power losses at the downstream branches are ignored and the voltage magnitude V_j at the receiving end of the branch is assumed to be V_0 [11], then (7) can be simplified as:

$$\left| \dot{I}_{ij} \right| = \frac{1}{V_0} \sqrt{\left(P_j + \sum_{k \in D_j} P_k \right)^2 + \left(Q_j + \sum_{k \in D_j} Q_k \right)^2} \tag{8}$$

D_j denotes the set of the downstream nodes of node j in the distribution network.

Setting the branch current at its upper limit, i.e., $\left| \dot{I}_{ij} \right| = I_{ij}^M$, the analytical expressions for the thermal boundaries of FOR can be derived as:

$$\left(\sum_{k=1}^{n} \alpha_k P_k \right)^2 + \left(\sum_{k=1}^{n} \beta_k Q_k \right)^2 = V_0^2 \left(I_{ij}^M \right)^2$$

$$\begin{cases} \alpha_k = \beta_k = 1, \text{ if } k \in D_j \text{ or } k = j \\ \alpha_k = \beta_k = 0, \text{ if } k \notin D_j \text{ and } k \neq j \\ \forall ij \in B \text{ (set of branches)} \end{cases} \tag{9}$$

From (9), the thermal boundaries are the quadratic form of the power injections at different nodes of the distribution network, which are different from the expressions of hyperplanes in the previous study [11]. It is worth noting that P_k and Q_k in (9) are defined as the power loading at node k in the deduction process. When defining them as the power injection at node k (i.e., the positive direction of active and reactive power at the node is defined as the injection direction), the form of the analytical expressions of thermal boundaries stays the same as (9). To be consistent with the definition of FOR in (1), P_k and Q_k in the expressions of thermal boundaries follow the definition of power injection in the following sections.

4. VALIDATION METHOD

To validate the obtained thermal boundaries of FOR of a given distribution network, a point-wise simulation method is used. The validation process is shown in Fig. 2.
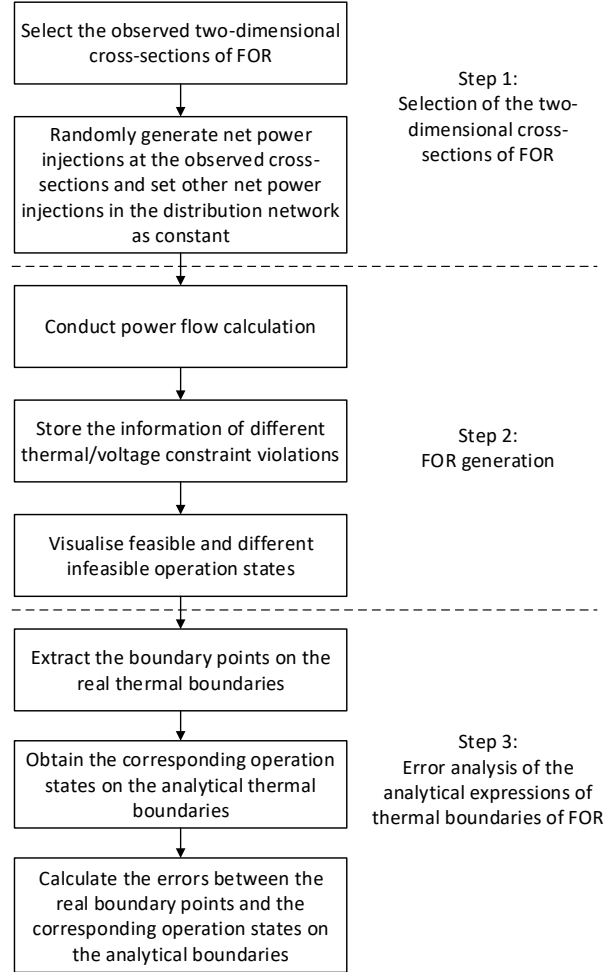

Fig. 2. Flow chart of the validation for the analytical expressions of thermal boundaries of FOR

Due to the high dimensionality of FOR, it is practical to compare the obtained analytical thermal boundaries with the real ones in the two-dimensional cross-sections. In this regard, two-dimensional cross-sections of FOR are selected in Step 1. In other words, for any targeted cross-section of FOR, two power injections (active or reactive power injections) are selected as variable, while other power injections are fixed.

In Step 2, FOR consists of all the obtained feasible operation states. The boundaries of FOR can be well approximated by the frontiers between the region containing feasible operation states and the regions containing infeasible operation states. The boundary points are approximated by the outermost feasible operation states of FOR, which are used for the error analysis in Step 3.

For Step 3, normalised mean absolute error (NMAE) and normalised maximum absolute error (NMaxAE) are used for quantifying errors:

$$NMAE = \frac{1}{m} \frac{\sum_{k=1}^{m} |e_k|}{S_{DN}} \times 100\% \qquad (10)$$

$$NMaxAE = \frac{\max |e_k|}{S_{DN}} \times 100\% \qquad (11)$$

e_k is the error between the kth boundary point and the analytical boundary. Since the error analysis is conducted in the two-dimensional cross-section of FOR, e_k is defined as horizontal error in abscissa direction and vertical error in ordinate direction respectively. The horizontal (or vertical) error is the difference between the kth boundary point and the corresponding point with the same ordinate value (or abscissa value) on the analytical boundary. m is the number of the selected boundary points (10 uniformly distributed boundary points on each thermal boundary are selected for error analysis in this study). S_{DN} is the rating of the distribution netowrk, which is suggested to use the rating of the main transformer or the first branch from the slack node of the network. The normalisation of the three error indices by dividing S_{DN} facilitates the comparison of the errors between distribution networks with different scales. .

5.   CASE STUDY

In this section, one feeder of the 11kV high-voltage underground network (HV UG) from the United Kingdom Generic Distribution System (UKGDS) [12] was used for the case study. The feeder studied is shown in Fig. 3. For simplification, the node 301 (slack node) and nodes 1100-1103 in [12] were numbered as node 1 and nodes 2 to 5 in Fig. 3. Active and reactive power injections at nodes 4 and 5 were variable, under the assumption that distributed generators are installed at node 4 and 5, with inverters capable of controlling the reactive power. The rating of the branch between nodes 2 and 3 (i.e., 6.82 MVA) is used as the rating of the feeder for error normalization (see (10) and (11)).
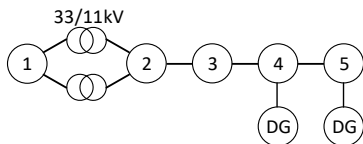

Fig. 3. The schematic diagram of the feeder selected from the 11kV UKGDS distribution network

The P_4-P_5, P_4-Q_5 and Q_4-Q_5 cross-sections of FOR of this feeder were selected to observe the hosting capacity of nodes 4 and 5. Except for the two observed active or reactive power injections in the selected cross-sections, other power injections at nodes 1-5 were in consistent with the data in the benchmark network[12].

Fig. 4 shows the selected three cross-sections of FOR for the feeder. For each cross-section, 50000 random samples of net power injections were used in the point-wise simulation and represented by dots with different colors according to their constraint violation conditions. The analytical thermal boundaries calculated using the methods in the previous study [11] and the present study are also shown in Fig. 4 as solid blue lines and red lines, respectively. Since voltage boundaries are not studied in this paper, the analytical voltage boundaries are not shown in Fig. 4.

It can be seen from Fig. 4 that the proposed analytical thermal boundaries (i.e. the red lines in Fig. 4) are very close to the real boundaries of FOR, thus being an effective way to reveal the whole picture of the hosting capacity of the network. The analytical thermal boundaries in P_4-P_5/Q_4-Q_5 cross-sections are straight lines with slopes of 0 or -1, while those in P_4-Q_5 cross-section are different. In the P_4-Q_5 cross-section, the analytical thermal boundaries for $I_{2,3}$ dn $I_{3,4}$ are circles, while the analytical thermal boundary for $I_{4,5}$ is a straight line with the slope of 0. The reason can refer to (9). In short, when both active and reactive power for the P-Q cross-section are at the downstream nodes (or the receiving end) of the observed branches, the analytical thermal boundaries for these branch currents will be circles. Otherwise, they will be straight lines with slopes of 0.

Table 1. Errors between the real thermal boundaries and the analytical thermal boundaries calculated using the methods in the previous study and the present study

Cross-sections	Error indices	Previous study [11]	Present study
		(Error indices in horizontal direction/%, Error indices in vertical direction/%)	
P_4-P_5	NMAE	(8, 10)	(2, 2)
	NMaxAE	(17, 17)	(5, 5)
P_4-Q_5	NMAE	(27, 118)	(2, 6)
	NMaxAE	(81, 201)	(8, 26)
Q_4-Q_5	NMAE	(50, 152)	(3, 4)
	NMaxAE	(103, 212)	(8, 8)

Furthermore, the error analysis results are listed in Table 1, which show that the errors of the analytical thermal boundaries in this study are significantly reduced and are small. Both in the horizontal and vertical directions, the NMAE are within 6%. Moreover, the

NMaxAE in P_4-P_5/Q_4-Q_5 cross-sections are less than 8%. However, it is notworthy that the NMaxAE values in the vertical direction of P_4-Q_5 cross-section can be 26%, though NMaxAE values in the horizontal direction are within 8%. The fact is that the circle boundaries in P_4-Q_5 cross-section are close to the real boundaries, i.e. the radial error is small. However, due to the topological characteristic of circles, the horizontal/vertical errors between some boundary points and the circle analytical boundaries can be larger than the radial error (for example 26% in this study).

From the results in Fig. 4 and Table 1, it can also be concluded that the proposed analytical thermal boundaries in this study are more accurate than those calculated using the method in the previous study, especially considering the impact of reactive power injections on the branch currents. From Table 1, the errors in P_4-Q_5 and Q_4-Q_5 crosss-sections obtained by the method in the previous study are large, indicating that the theory in [11] needs to be extended when independent reactive power injections are considered.
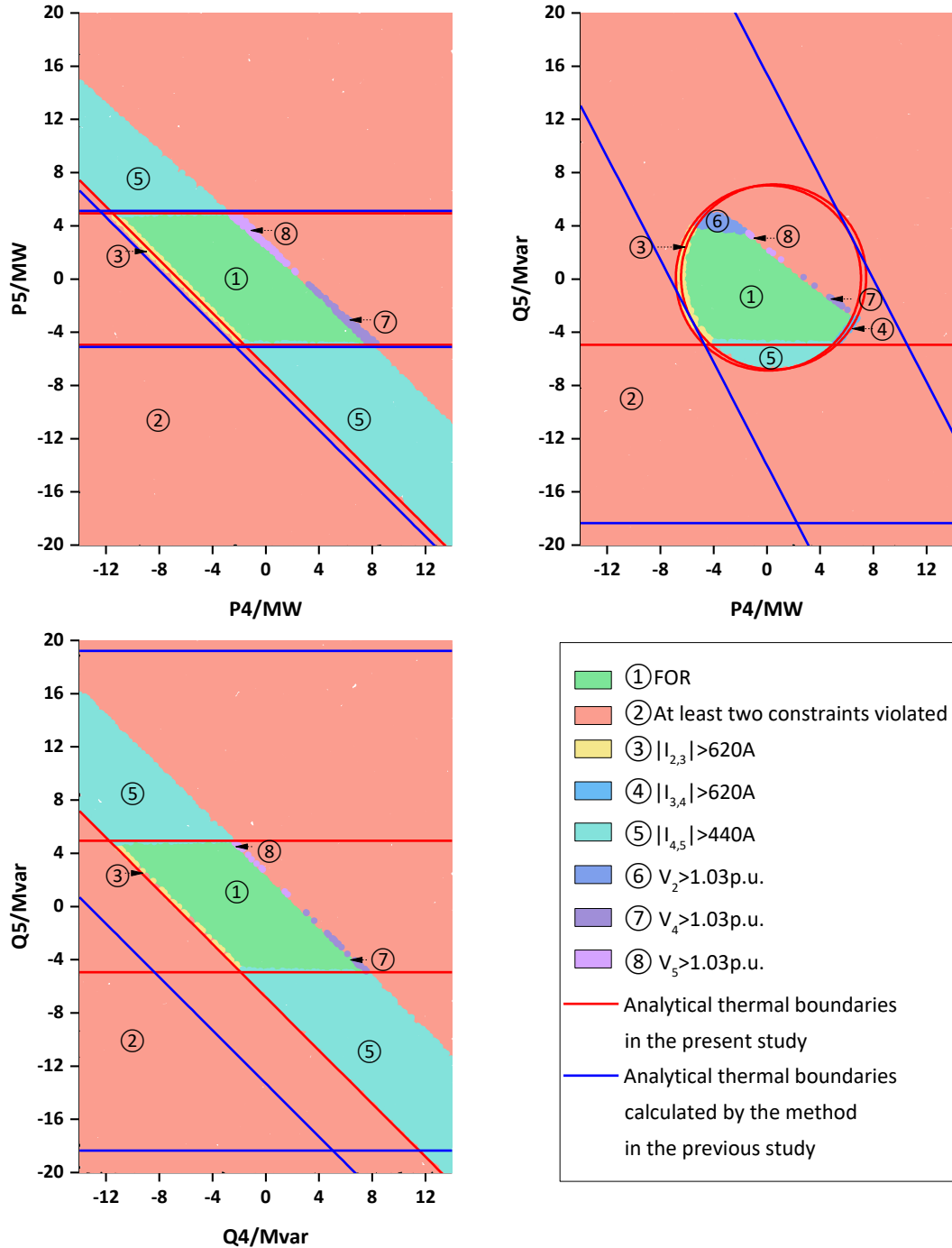

Fig. 4. P_4-P_5, P_4-Q_5 and Q_4-Q_5 cross-sections of FOR of the feeder

6. CONCLUSION

In this paper, feasible operation region is proposed to depict the whole picture of the hosting capacity of distribution networks. This paper focuses on the thermal constraints of distribution networks. The analytical expressions of thermal boundaries of FOR are in the quadratic form of the power injections at different nodes of the distribution network. In P-P/Q-Q cross-sections, the analytical thermal boundaries are straight lines with slopes of 0 or -1, while those in P-Q cross-sections are circles or straight lines with slopes of 0. The different features of the analytical thermal boundary for an observed branch in the two-dimensional cross-sections depend on whether the observed power injections are at the downstream nodes (or the receiving end) of the observed branch.

From the results of the case study, the proposed analytical expressions of thermal boundaries are able to well approximate the real thermal boundaries of FOR. The absolute horizontal/vertical errors between the proposed analytical thermal boundaries and the real thermal boundaries were controlled within 6% in the two-dimensional cross-sections studied. The maximum absolute errors are less than 8% in the observed P-P/Q-Q cross-sections, while the largest 26% maximum absolute error exists in the observed P-Q cross-section. Compared with the hyperplane expressions in the previous study, the proposed analytical expressions of thermal boundaries of FOR in this paper are more accurate and show great advantages when considering the impact of reactive power injections.

REFERENCE

[1] Diaz, D, Kumar, A, Deboever, J, Grijalva, S, Peppanen, J, Rylander, M, Smith, J. Scenario-selection for hosting capacity analysis of distribution feeders with voltage regulation equipment. C 2019 IEEE Power & Energy Society Innovative Smart Grid Technologies Conference (ISGT). IEEE, 2019: 1-5.

[2] Ding, F, Mather, B. On distributed PV hosting capacity estimation, sensitivity study, and improvement. J IEEE Transactions on Sustainable Energy 2016; 8:1010-1020.

[3] Thomas, L J, Burchill, A, Rogers, D J, Guest, M, Jenkins, N. Assessing distribution network hosting capacity with the addition of soft open points. 2016.

[4] Alturki M T. Hosting capacity calculations in power systems. 2014.

[5] AlAlamat F. Increasing the hosting capacity of radial distribution grids in Jordan. 2015.

[6] Wang, S, Chen, S, Ge, L, & Wu, L. Distributed generation hosting capacity evaluation for distribution systems considering the robust optimal operation of OLTC and SVC. J IEEE Transactions on Sustainable Energy, 2016; 7:1111-1123.

[7] Mina Mirbagheri S, Falabretti D, Ilea V, Merlo M. Hosting capacity analysis: a review and a new evaluation method in case of parameters uncertainty and multi-generator. C 2018 IEEE International Conference on Environment and Electrical Engineering and 2018 IEEE Industrial and Commercial Power Systems Europe (EEEIC/I and CPS Europe). Institute of Electrical and Electronics Engineers Inc; 2018:1-6.

[8] Le Baut J, Zehetbauer P, Kadam S, Bletterie B, Hatziargyriou N, Smith J, Rylander M. Probabilistic evaluation of the hosting capacity in distribution networks. C 2016 IEEE PES innovative smart grid technologies conference Europe (ISGT-Europe). IEEE; 2016:1-6.

[9] Yu Y, Liu Y, Qin C, Yang T. Theory and method of power system integrated security region irrelevant to operation states: An introduction. J Engineering, 2020; 6:754-777.

[10] Xiao J, Zu G, Wang Y, Zhang X, Jiang X. Model and observation of dispatchable region for flexible distribution network. J Applied Energy, 2020; 261:114425.

[11] Yang T, Yu Y. Steady-state security region-based voltage/var optimization considering power injection uncertainties in distribution grids. J IEEE Transactions on Smart Grid, 2018; 10:2904-2911.

[12] Centre for Sustainable Electricity and Distributed Generation. United Kingdom Generic Distribution System. [Online]. Available: https://github.com/sedg/ukgds.